Article

Long-Range Stabilization of Anthrax Protective Antigen upon Binding to CMG2

Vennela Mullangi,[†,‖] Sireesha Mamillapalli,[⊥] David J. Anderson,[‖] James G. Bann,*[⊥,#] and Masaru Miyagi*[†,‡,§]

[†]Case Center for Proteomics and Bioinformatics, [‡]Department of Pharmacology, and [§]Department of Ophthalmology and Visual Sciences, Case Western Reserve University, Cleveland, Ohio 44106, United States

[‖]Department of Chemistry, Cleveland State University, Cleveland, Ohio 44114, United States

[⊥]Department of Chemistry, Wichita State University, Wichita, Kansas 67260, United States

[#]University of Kansas School of Medicine-Wichita, Wichita, Kansas 67214, United States

S *Supporting Information*

ABSTRACT: Protective antigen (PA) mediates entry of edema factor (EF) and lethal factor (LF) into the cytoplasmic space of the cells through the formation of a membrane-spanning pore. To do this, PA must initially bind to a host cellular receptor. Recent mass spectrometry analysis of PA using histidine hydrogen−deuterium exchange (His-HDX) has shown that binding of the von Willebrand factor A (vWA) domain of the receptor capillary morphogenesis protein-2 (CMG2) lowers the exchange rates of the imidazole C_2 hydrogen of several histidines, suggesting that receptor binding decreases the structural flexibility of PA. Here, using His-HDX and fluorescence as a function of denaturant, and protease susceptibility, we show that binding of the vWA domain of CMG2 largely increases the stability of PA and the effect reaches up to 70 Å from the receptor binding interface. We also show that the pK_a values and HDX rates of histidines located in separate domains change upon receptor binding. These results indicate that when one end of the protein is anchored, the structure of PA is tightened, noncovalent interactions are strengthened, and the global stability of the protein increases. These findings suggest that CMG2 may be used to stabilize PA in future anthrax vaccines.
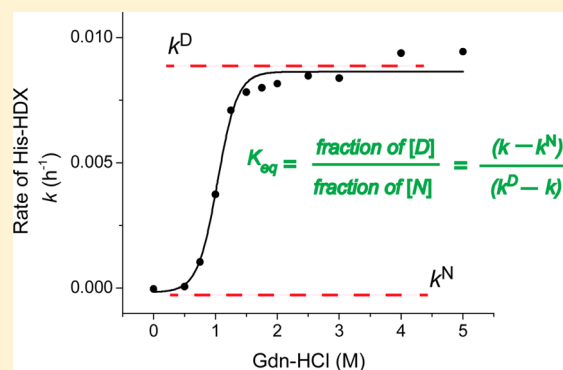
The anthrax protective antigen (PA) is the receptor binding component of the anthrax toxin, a complex of proteins that mediates the pathogenicity of anthrax disease. After binding to the receptor, PA undergoes proteolytic processing by a furin-like protease, which cleaves off the N-terminal 167 amino acid residues of PA within domain 1 (residues 1−258), termed PA_{20}.[1] PA_{20} subsequently dissociates and leaves behind domain 1′ (residues 168−258) and the three remaining domains, constituting a 63 kDa fragment (PA_{63}). This fragment then oligomerizes into either a heptameric[2] or octameric[3] structure termed the prepore. Binding of PA to the receptor hijacks the host cell receptor to allow targeting of the other two components of the anthrax toxin, lethal factor (LF) and edema factor (EF), to the host cell surface. Once the prepore has formed, the toxin is internalized by receptor-mediated endocytosis.

The structural details of PA binding to the host cell receptor capillary morphogenesis protein-2 (CMG2) are known, bound to either the monomeric 83 kDa PA[4] or the heptameric prepore.[2] Both structural and biochemical studies of the PA−CMG2 complex indicate that the binding interface is comprised of domain 4 and a small loop from domain 2 ($2\beta3−2\beta4$ loop),

which inserts into a groove on the surface of CMG2 (Figure 1).[2,4−6] The binding affinity between PA and CMG2 is very high ($K_d \sim 200$ pM)[7] and increases at acidic pH.[8] At the same time, receptor binding has been shown to improve the stability of the heptameric form of PA to pH and to facilitate the internalization of the toxin-bound prepore.[9,10] Our recent NMR study of PA labeled with 5-fluorotryptophan also suggested that receptor binding significantly stabilizes PA to both pH and temperature.[11]

To further investigate the changes in stability of PA upon CMG2 binding, we used a histidine hydrogen−deuterium exchange (His-HDX) method,[12] which monitors the slow rate of HDX of the C_2 hydrogen of the imidazole group of histidine, and followed the rate of HDX as a function of increasing concentrations of guanidinium hydrochloride (Gdn-HCl).[13] Thus, using this method, we can measure the equilibrium unfolding of specific histidine residues within the protein. There are 10 histidine residues in PA that are scattered
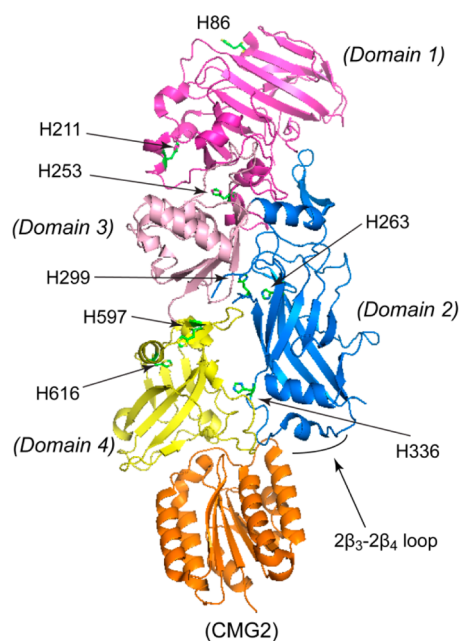
Figure 1. Structure of the PA−CMG2 complex (PDB entry 1T6B). Eight histidine residues are shown (green sticks). Domain 1, Ser15−Ala258 (magenta); domain 2, Tyr259−Thr487 (blue); domain 3, Thr488−Arg595 (pink); domain 4, Phe596−Ile734 (yellow); vWA domain of CMG2 (orange). All the histidine residues in PA except His304 and His310 are shown. His304 and His310 are not observed in the structure. The $2\beta3-2\beta4$ loop of domain 2 is also indicated.

throughout the molecule, one in the PA_{20} domain, two in domain 1′, five in domain 2, and two in domain 4. Herein, we show that receptor binding leads to a significant shift in the concentration of Gdn-HCl required for full HDX (unfolding) of histidines located in separate domains, suggesting that receptor binding has a global effect on the thermodynamic stability of the protein. These studies are corroborated using fluorescence, in which we were able to probe selectively fluorescence changes in PA using a 4-fluorotryptophan-labeled von Willebrand factor A (vWA) domain of CMG2, which is nonfluorescent. His-HDX-MS also allowed us to determine the pK_a and more accurate solvent accessibilities of the histidines in the presence and absence of the receptor and reveal differences in the microenvironment around the histidine residues as a consequence of receptor binding. Our results indicate that receptor binding has a profound long-range impact on the stability and structure of PA, suggesting that, with a limit on hingelike motions between domain 2 and domain 4, the protein can be made to be significantly more stable. Because PA is the major antigenic component of the current anthrax vaccine, our studies would indicate that addition of CMG2 to a vaccine formulation could improve the stability and overall efficacy of the vaccine.

■ MATERIALS AND METHODS

Materials. Deuterium oxide (D_2O, 99%) was purchased from Cambridge Isotope laboratories (Andover, MA), and guanidine hydrochloride (Gdn-HCl), deuterium chloride (DCl), and sodium deuteroxide (NaOD) were from Sigma-Aldrich (St. Louis, MO). Lys-C was purchased from Wako Chemicals USA (Richmond, VA); chymotrypsin and thermolysin were from Sigma-Aldrich, and Glu-C was from Worthington Biochemical (Lakewood, NJ). All other chemicals

and materials used were either reagent grade or of the highest quality commercially available.

Protein Expression and Purification. PA and the vWA domain of CMG2, encoding residues 38−218, were expressed and purified as described previously.[14−16] Labeling of CMG2 with 4-fluorotryptophan was conducted using the tryptophan auxotroph DL41 (provided as a gift from the Yale *E. coli* Genetic Stock Center). 4-Fluorotryptophan was purchased from Gold Biotechnology (St. Louis, MO).

Unfolding Experiments Followed by His-HDX. PA alone (0.5 nmol) and the PA−CMG2 complex (0.5 nmol of PA and 2.5 nmol of CMG2) were incubated in 100 μL of 100 mM HEPES (pH* 7.5) made with D_2O containing 1 mM $MgCl_2$ and various concentrations of Gdn-HCl for 48 h at 37 °C. The pH* of the buffer was adjusted with diluted NaOD with a Solution Analyzer model 4603 instrument (Amber Science, Eugene, OR) equipped with a glass AgCl electrode (model 476086, Nova Analytics, Woburn, MA). The reported pH* values are direct pH meter readings of the D_2O buffer solutions calibrated with standard buffer solutions made with H_2O and are uncorrected for the isotope effect at the glass electrode. The reaction was stopped by adding 10 μL of formic acid, and the protein was freed from the salts using an Ultra Micro Spin C4 column (Nest Group, Southboro, MA) following the manufacturer's instructions and dried in a Speed Vac.

The protein was then redissolved in 60 μL of 100 mM ammonium bicarbonate and digested by 2 μg of Lys-C for 30 min at 25 °C. The reaction was stopped by adding 10 μL of formic acid, and the digest was divided into three parts and then dried in a Speed Vac. Two parts were further digested, one part by 1 μg of Glu-C for 30 min and other part by 1 μg of chymotrypsin for 30 min. The resulting three digests were dried in a Speed Vac and redissolved in 30 μL of 0.1% trifluoroacetic acid (TFA). The three digests at particular Gdn-HCl concentrations were mixed and analyzed by liquid chromatography and tandem mass spectrometry (LC−MS/MS) using a Qstar quadrupole/time-of-flight mass spectrometer (Applied Biosystems-MDS Sciex, Foster City, CA) equipped with a TurboIonSpray ion source. The protein digests were injected into a reverse-phase C18 column (500 mm × 0.1 mm, Waters); the peptides were chromatographed using a linear gradient of acetonitrile from 2 to 50% in aqueous 0.1% formic acid over a period of 40 min at a rate of 30 μL/min, and the elute was directly introduced into the mass spectrometer. The total ion current was obtained in the mass range of m/z 400−2000 in the positive ion mode with an acquisition time of 1 s for each scan.

The pseudo-first-order rate constant (k) of the HDX reaction was determined by monitoring changes in the ratios of the M + 1/M isotopic peak of a given peptide before (time zero) and after (time t) the HDX reaction, and fitting the data to a first-order rate equation,[17] and the values were corrected upward to offset the decreased solvent concentration caused by the volume effect of Gdn-HCl. The relationship between solvent concentration and Gdn-HCl concentration was experimentally determined, from which the correction factor to correct the rate constant of the HDX reaction in Gdn-HCl solutions was obtained (text and Figure S1 of the Supporting Information). The corrected HDX rate was plotted against the concentration of Gdn-HCl. From the plot, the midpoint (C_m) of the Gdn-HCl-induced unfolding transition was estimated by fitting the denaturation curve to a two-state model. The free energy change ($\Delta G°$) in PA denaturation was estimated from the plot
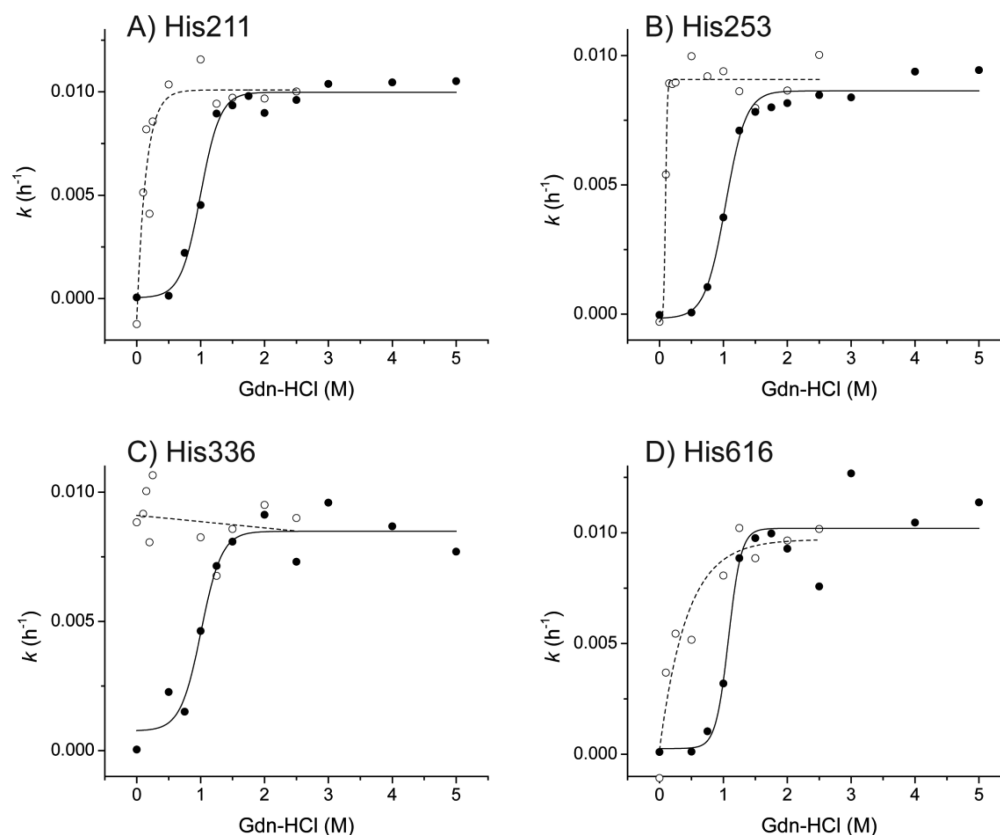
Figure 2. Gdn-HCl denaturation curves of PA alone (---) and PA complexed with CMG2 (—). PA and the PA–CMG2 complex were incubated in 100 mM HEPES (pH* 7.5) at 37 °C for 48 h in various concentrations of Gdn-HCl. After the incubation, the protein was digested and the resulting peptides were analyzed by LC–MS/MS. The HDX rates of four histidine residues, His211 (A), His253 (B), His336 (C), and His616 (D), were monitored to follow the Gdn-HCl-induced denaturation of PA.

by calculating the equilibrium constant (K_{eq}) of denature/native protein at each Gdn-HCl concentration as follows.

$$K_{eq} = \frac{\text{fraction of } [D]}{\text{fraction of } [N]} = \frac{k - k^N}{k^D - k}$$

where k is the first-order His-HDX rate constant at a specific Gdn-HCl concentration, k^N is the k for the native protein (k at 0 M Gdn-HCl), and k^D is the k for the fully denatured protein (can be obtained from the plateau of the sigmoidal curve). The K_{eq} value was used to determine the free energy change of denaturation at each Gdn-HCl concentration with the equation

$$\Delta G° = -RT \ln K_{eq}$$

where R is the gas constant and T is the absolute temperature in kelvin. By plotting the $\Delta G°$ values against the concentrations of Gdn-HCl and extrapolating the fitted line to 0 M Gdn-HCl, we obtained $\Delta G°_{water}$ in the absence of Gdn-HCl.

Unfolding Experiments Followed by Fluorescence Spectroscopy. PA alone and PA (1 μmol) complexed with 4-fluorotryptophan-labeled CMG2 (4-FTrpCMG2, 2 μmol) in 100 mM HEPES (pH 7.5) containing 1 mM MgCl₂ and various concentrations of Gdn-HCl were placed in a Cary-Eclipse fluorimeter, and the fluorescence emission spectra were recorded at 20 °C by exciting the tryptophan residues in PA at 295 nm and monitoring the emitted light at 334 nm. The data were fit to a three-state transition in the absence of CMG2 as described previously.[15]

Pulse Proteolysis Assay. The method described by Young and co-workers was used to conduct the pulse proteolysis

experiment.[18] PA (100 μg, 6 μM) or PA with 48 μg (12 μM) of CMG2 was incubated overnight at room temperature in 200 μL of 20 mM Tris buffer (pH 8.0) containing 150 mM NaCl, 10 mM CaCl₂, and 1 mM MgCl₂. The next day, 20 μL of 5 mg/mL thermolysin prepared in 2.5 M NaCl and 10 mM CaCl₂ was added to the 200 μL of PA and PA–CMG2 complex samples and incubated at room temperature for various periods of up to 120 min. Aliquots (15 μL) were withdrawn at the different time points, to which 5 μL of 50 mM EDTA and 4 μL of 6× SDS–PAGE sample buffer were added to stop the proteolysis. The solution was then boiled for 5 min, and 15 μL of the solution was run on a 15% SDS–PAGE gel.

pH* Titration Studies. PA (0.5 nmol) and the PA–CMG2 complex (0.5 nmol of PA and 2.5 nmol of CMG2) were placed in 100 μL of buffer with different pH* values (4.5–9.0) that contains 20 mM CHES, 20 mM HEPES, 20 mM MES, 50 mM NaCl, and 1 mM MgCl₂ and incubated for 50 h at 37 °C. The pH* of the buffer was adjusted with diluted DCl or NaOD. The reaction was stopped by adding 5 μL of formic acid, and the protein was freed from the buffer salts using an Ultra Micro Spin C4 column (Nest Group) according to the manufacturer's instructions and dried in a Speed Vac. The protein was redissolved in 100 mM ammonium bicarbonate and digested with Lys-C alone, a combination of Lys-C and Glu-C, or a combination of Lys-C and chymotrypsin as described above. The resulting digests were dried in a Speed Vac, redissolved in 0.1% TFA, and then analyzed by LC–MS/MS using an LTQ-Orbitrap XL mass spectrometer as described previously.[17] The pseudo-first-order rate constant (k) of the HDX reaction was

determined as described above, and the k values were plotted as a function of pH*, from which the pK_a of each histidine residue and the half-life ($t_{1/2}$) of the HDX reaction were determined.[17]

Structural Analysis. A comparison of protein structures was performed using PyMOL (Molecular Graphics System software, DeLano Scientific, Palo Alto, CA). The structural data of PA (PDB entry 3Q8B) and the PA−CMG2 complex (PDB entry 1T6B) deposited in the Protein Data Bank were used in the comparison. The same structural data were used to obtain the ASA (solvent accessible surface are) values for the C_2 atoms of the histidine residues using GETAREA.[19]

■ RESULTS AND DISCUSSION

Stability of PA and PA Bound to CMG2. To investigate how the stability of PA changes upon binding to CMG2, we conducted Gdn-HCl-induced equilibrium unfolding experiments on PA alone and PA complexed with CMG2, using His-HDX-MS. Histidine residues in a protein that are protected (to at least a certain extent) from the solvent become exposed to solvent upon unfolding of the protein caused by increasing concentrations of Gdn-HCl, which subsequently increases the magnitude of HDX rates for the histidine residues as the protein unfolds. The histidine residues we monitored were His211, His253 (domain 1′), His336 (domain 2), and His616 (domain 4). Four peptides containing these four histidine residues, each containing one histidine residue, were detected by LC−MS/MS (Table S1 of the Supporting Information), and their precursor ion spectra were used to calculate the pseudo-first-order rate constants (k) for their HDX reactions.

During the study, it became apparent that the HDX rates obtained in the Gdn-HCl solution must be corrected upward. This is because the concentration of water in a highly concentrated Gdn-HCl solution (e.g., 5 M Gdn-HCl) is significantly lower than the concentration of water in a solution without Gdn-HCl. This means that the amount of a heavy water molecule (D_2O) available in such a solution in a defined volume is significantly small, causing us to underestimate the HDX rates. We determined the relationship between the water and Gdn-HCl concentrations in various concentrations of Gdn-HCl solutions, from which an equation to correct upward the experimentally obtained HDX rates was obtained (see the Supporting Information). All the HDX rates measured in Gdn-HCl solutions were corrected using this equation.

In Figure 2, Gdn-HCl-induced denaturation curves of PA alone (dashed line) and PA complexed with CMG2 (solid line) monitored at these four histidine residues are shown. PA denatured rapidly at very low Gdn-HCl concentrations, which prevented determination of the C_m value (midpoint of the Gdn-HCl-induced unfolding transition) for PA alone accurately. Nevertheless, we estimated the C_m values by visual inspection, which were ≈0.2, ≈0.2, and ≈0.5 M for His211, His253, and His616, respectively (Table 1). The C_m value at His336 could not be determined, because this histidine is already exposed well to solvent in the native structure as indicated by the high HDX rate for this residue at 0 M Gdn-HCl (Figure 2C, dashed line). The C_m values for PA complexed with CMG2 were ∼2−5-fold larger than those for PA alone (approximately 1 M at all four histidine residues) as shown in Table 1. The data in Figure 2 are representative of three separate experiments. The values of C_m (molar) for the PA−CMG2 complex were reproducible to ±12%. His211 is ∼70 Å from the binding interface. Thus, our data indicate that PA is stabilized throughout most of the protein by receptor binding, and the unfolding of these

Table 1. Transition Midpoints and Stabilities for the Gdn-HCl-Induced Unfolding of PA and PA Complexed with CMG2

		PA		PA−CMG2	
residue	domain	C_m (M)	ΔG (kcal mol^{-1})	C_m (M)^a	ΔG (kcal mol^{-1})
His211	1	≈0.2	−	1.00 ± 0.04	5.17
His253	1	≈0.2	−	1.03 ± 0.04	4.36
His336	2	−	−	1.01 ± 0.08	4.37
His616	4	≈0.5	−	1.08 ± 0.06	5.11

^{a}The standard errors are associated with the sigmoidal curve fitting.

residues, despite being located in different domains, occurs at concomitant Gdn-HCl concentrations. In addition to the C_m values, we were able to estimate the standard state Gibbs free energy values from linear extrapolation of the His-HDX values as a function of denaturant, in the presence of CMG2. The calculated $\Delta G°$ values were approximately 4−5 kcal mol^{-1} at all four histidine residues (Table 1), suggesting that all are stabilized to a similar extent.

Previous fluorescence and ^{19}F NMR unfolding experiments in urea have shown that PA unfolds in two transitions, the first transition being assigned to the unfolding of domains 1′−4 and the second transition being mainly due to the PA$_{20}$ domain, which after cleavage with furin can freely dissociate and is stable on its own.[11,14,15] Here, we followed the Gdn-HCl-induced unfolding of PA by fluorescence in the presence of CMG2, where we have labeled CMG2 with 4-fluorotryptophan (4-FTrp). This effectively eliminates the fluorescence contribution from the sole tryptophan (Trp59) of CMG2, because 4-FTrp is a nonfluorescent analogue of tryptophan (see the inset of Figure 3).[20] The structure of CMG2 is largely unchanged upon labeling, as evidenced by the far-UV CD spectrum of wild-type (WT) CMG2 and 4-FTrpCMG2 (Figure S2 of the Supporting Information). Gdn-HCl-induced denaturation curves of PA alone and PA complexed with 4-FTrpCMG2 are shown in
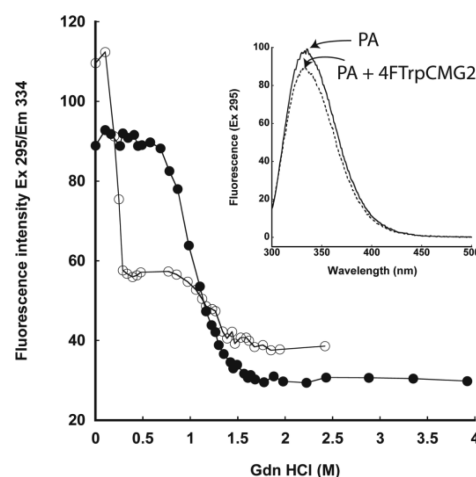

Figure 3. Gdn-HCl denaturation curves of PA alone (○) and PA complexed with CMG2 (●). The fluorescence emission spectra of PA alone and PA complexed with 4-FTrpCMG2 in 100 mM HEPES (pH 7.5) containing 1 mM MgCl$_2$ and various concentrations of Gdn-HCl were recorded by exciting the tryptophan residues in PA at 295 nm and monitoring the emitted light at 334 nm. The inset shows fluorescence emission spectra of PA and PA complexed with 4-FTrpCMG2.

Figure 3. As we observed previously in urea, PA undergoes two transitions by fluorescence, which we again have assigned to the unfolding of domains 1′−4 constituting the PA$_{63}$ region of PA at a low Gdn-HCl concentration (∼0.2 M) and to the PA$_{20}$ domain at higher (∼1.3 M) Gdn-HCl concentrations.[11] In the presence of CMG2, we observed one single transition at a C_m of ∼1.3 M, suggesting that domains 1′−4 were significantly stabilized by receptor binding. We did not see a further increase in stability above that of the PA$_{20}$ domain, suggesting that receptor binding largely stabilizes residues up to the PA$_{20}$ region. In any case, these results agree well with the results obtained with the His-HDX-MS method.

Protease Susceptibility of PA and PA Bound to CMG2. Resistance to proteolysis is an effective way to probe accessibility to unfolded conformations in a protein, and we hypothesized that CMG2 binding would "tighten" the structure of the protein and decrease the rate of proteolytic degradation.[18] To test whether binding of CMG2 stabilizes PA against proteolysis, we incubated PA and the PA−CMG2 complex (1:2 ratio) at room temperature with thermolysin for different periods of time and analyzed the resulting reactions by SDS−PAGE. In the case of PA alone, the undigested PA band disappeared within 30 s and appeared to be cleaved into two fragments (50 and 40 kDa) (Figure 4A). The two fragments,
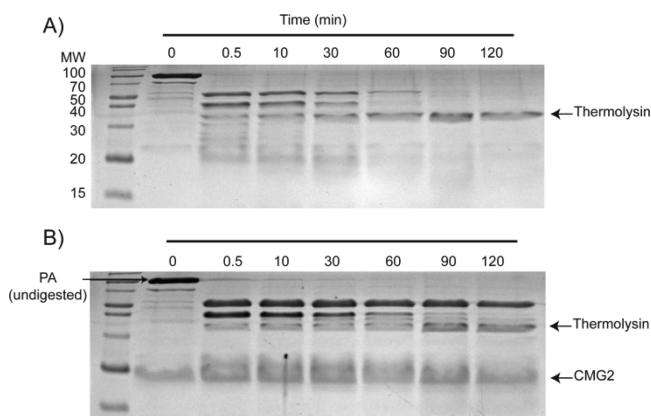

Figure 4. Proteolysis of PA alone (A) and PA complexed with CMG2 (B) by thermolysin. PA or PA complexed with CMG2 (100 μg) was incubated with 100 μg of thermolysin at room temperature for various periods of time (up to 120 min). Aliquots were withdrawn at the different time points and run on a 15% SDS−PAGE gel.

however, did not last long, fading away within 60 min. In the case of PA complexed with CMG2, the undigested band similarly disappeared within 30 s; however, the generated 50 kDa band was clearly seen even after incubation for 120 min (Figure 4B). The 40 kDa band faded away also within 60 min. To determine the thermolysin cleavage site, we analyzed the PA−CMG2 complex treated with thermolysin by LC−MS. We observed one major peak, in addition to the peaks that correspond to thermolysin and CMG2. The major peak gave a mass of 47007.4 Da and likely encompasses the 50 kDa band. The molecular weight matched well to the calculated molecular weight of the C-terminal portion of PA, Ile326−Gly745 (47002.5 Da). Thus, the 50 kDa band is likely the C-terminal portion of PA produced by the hydrolysis between Asp315 and Ile316. The site has a preferred sequence recognized by this protease (X-Ile, X-Leu, X-Val, or X-Phe, where X is any amino acid)[21] and falls within the flexible region (His304−Ser319)

that cannot be observed in the crystal structures of PA or the PA−CMG2 complex.[4,8,22] The thermolysin resistance of the C-terminal fragment suggests that CMG2 remains bound to the C-terminal fragment after the proteolytic cleavage, thus providing continued resistance against thermolysin.

pK_a Values and His-HDX Rates. In previous studies, we compared, using His-HDX-MS, the effect of CMG2 binding on the rate of exchange at pH* 9.5;[14] however, we were unable to determine the pK_a values of the histidines, which this technique also allows. Therefore, in a manner similar to our previous work, we conducted a pH* titration study on PA alone and the PA−CMG2 complex using His-HDX-MS. The protein was deuterated in different pH* buffers (4.5−9.0), digested, and then analyzed by LC−MS/MS. All 10 histidine residues were detected in different peptides (Table S2 of the Supporting Information). The rate constants (k) for HDX of those histidine residues were calculated directly from their precursor ion spectra. The obtained k values as a function of pH* for six histidine residues (His86, His263, His304, His310, His336, and His597) are shown in Figure 5. We could not obtain interpretable sigmoid curves for His211, His253, His299, and His616 because of their slow HDX rates. All the histidine residues in Figure 5 gave simple sigmoid curves corresponding to a single pK_a except for His263 in PA, which showed a steep rise above pH* 7 without an explicit inflection point (Figure 5B, dashed line). We believe this curve reflects the increased local conformational fluctuation and reversible unfolding around this residue at alkaline pH*, causing the histidine residue to be exposed more to solvent, rather than reflecting the acid dissociation of this residue. The phenomenon was not observed for the same residue in the PA−CMG2 complex (Figure 5B, solid line), suggesting that binding to the receptor increases the stability of this region against alkaline pH*. The k value for His336 (Figure 5E, solid line) in the PA−CMG2 complex was too low to produce interpretable sigmoidal curves.

Measured pK_a values from the sigmoid curves for His86, His304, His310, His336, and His597 are shown in Table 2. Significant changes in pK_a for His86 and His310 were observed, which was surprising given that His86 is >90 Å from the binding interface. In general, the pK_a of histidines depends on several factors; however, the lower the pK_a (<6), the stronger the tendency to be buried and uncharged at neutral pH, while a higher pK_a (>7.5) generally reflects the greater potential for charge−charge interactions. The pK_a of His86 decreased 0.61 pH unit upon binding to CMG2 (from ∼6.7 to 6.1), while the pK_a of His310 increased 1.68 pH units. In previous work, we compared the distances of the histidine residues to potential hydrogen bond donors and/or acceptors and in general found that the distances became shorter in the presence of CMG2.[14] Indeed, for His86, the distance to the Gln121 backbone carbonyl decreases from 3.43 to 3.07 Å, and this decreased distance is likely reflected in a slight lowering of the pK_a. In contrast to that of His86, the pK_a of His310 increased 1.68 pH units upon binding to CMG2, from 6.26 to 8.06. We are not able to offer an interpretation of the observed pK_a change of this residue because His310 is not observed in the crystal structures of PA and the PA−CMG2 complex. However, the increased pK_a suggests that one or more acidic side chains (e.g., Asp or Glu) may come close to His310 upon binding to CMG2. Indeed, Glu308, Glu302, and Asp315 are local candidates for interacting with His310.

In addition to His86 and His310, we were able to determine the pK_a values of His263 (for only the PA−CMG2 complex),
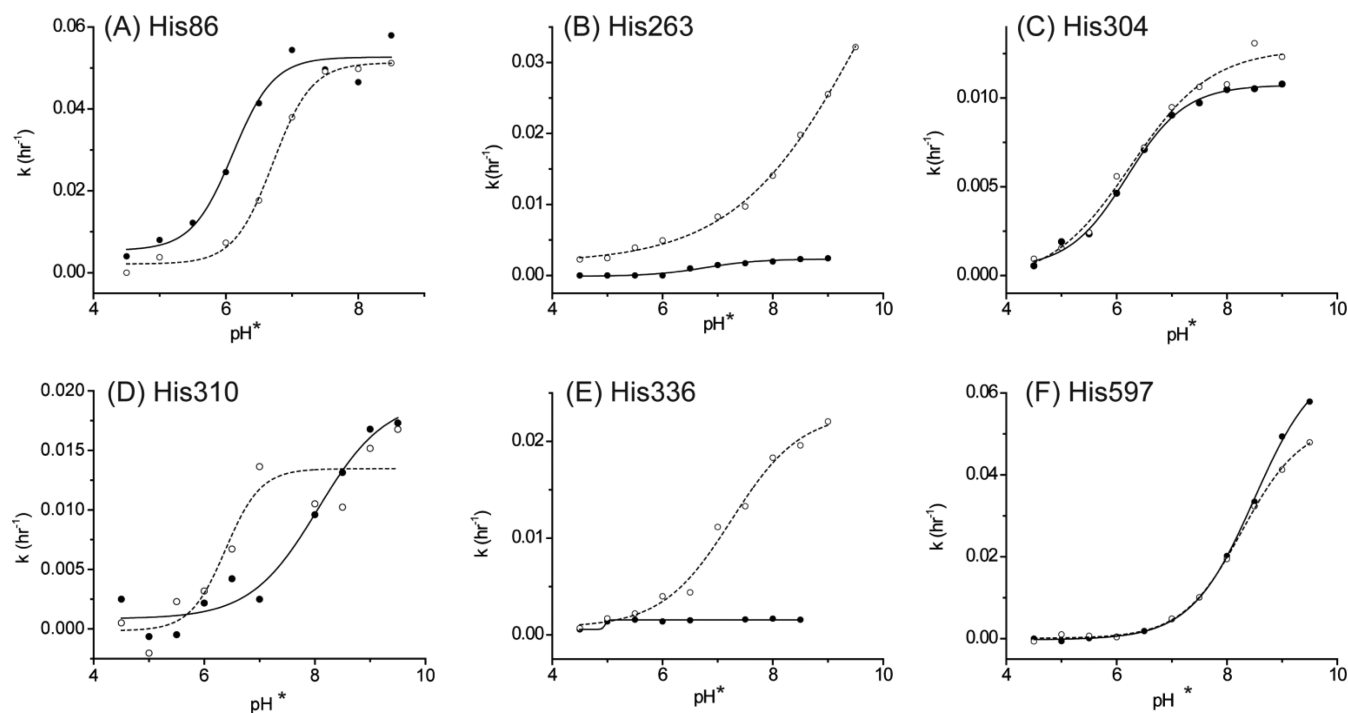
Figure 5. pH* dependence of the k for HDX at the imidazole group of six histidine residues in PA alone (---) and PA complexed with CMG2 (—). PA and the PA−CMG2 complex were incubated at different pH* values (4.5−9.0) at 37 °C for 50 h. After the incubation, the protein was digested and the resulting peptides were analyzed by LC−MS/MS. The pH* dependencies of the k values for HDX for (A) His86, (B) His263, (C) His304, (D) His310, (E) His336, and (F) His597 are shown.

Table 2. pK_a and $t_{1/2}$ Values of Histidine Residues in PA and the PA−CMG2 Complex[a]

residue	domain	pK_a		$t_{1/2}$ (day)	
		PA	PA−CMG2	PA	PA−CMG2
His86	1	6.71 ± 0.04	6.10 ± 0.12	0.57 ± 0.01	0.55 ± 0.03
His211	1	ND[b]	ND[b]	20.77^c	24.11^c
His253	1	ND[b]	ND[b]	$>50^c$	$>50^c$
His263	2	ND[b]	6.77 ± 0.15	1.13^c	12.45 ± 0.85
His299	2	ND[b]	ND[b]	7.17^c	7.95^c
His304	2	6.26 ± 0.18	6.19 ± 0.06	2.26 ± 0.12	2.71 ± 0.07
His310	2	6.38 ± 0.25	8.06 ± 0.29	2.14 ± 0.20	1.50 ± 0.02
His336	2	7.25 ± 0.13	ND[b]	1.26 ± 0.09	13.98^c
His597	4	8.28 ± 0.04	8.49 ± 0.04	0.55 ± 0.01	0.42 ± 0.01
His616	4	ND[b]	ND[b]	33.48^c	33.79^c

[a]The standard errors are associated with the sigmoidal curve fitting. [b]The pK_a could not be determined mainly because of the slow HDX rate. [c]Calculated from k at pH 9.0 instead of using k_{max}, because k_{max} could not be obtained because of the lack of an interpretable sigmoidal curve.

His304, His336 (for only PA), and His597. The pK_a of His263 in the PA−CMG2 complex was determined to be 6.77, which is close to the intrinsic pK_a value of a histidine residue ($pK_a \approx$ 6.5),[12] suggesting little electrostatic influence of the neighboring groups on this residue. The pK_a of His336 in PA was slightly higher (7.25) than the intrinsic pK_a value of the histidine residue, suggesting there is a moderate influence of the electron-donating group(s) around this residue. The pK_a values of His597 in both PA and the PA−CMG2 complex were shifted almost 2 pH units toward alkaline values (≥ 8), indicating there is a negatively charged group(s) in the proximity of this histidine. As expected, the imidazole ring of His597 is in the proximity of the carboxyl group of Asp608 and likely forms a salt bridge to this residue, in agreement with the crystal structure.[14]

We previously reported the half-lives $[t_{1/2} \text{ (days)}]$ of the HDX reactions of histidine residues in PA.[14] Those $t_{1/2}$ values were calculated from the HDX rates obtained at a single pH* (9.5). In this study, we calculated the $t_{1/2}$ values from the maximal rate constant (k_{max}) obtained from the plateau to the alkaline side of the sigmoid titration curve as described previously.[17] The $t_{1/2}$ values calculated in this way are considered to be more accurate, because they are calculated from the k_{max} values obtained from the pH* titration curves fit to multiple data points. The $t_{1/2}$ values for His86, His263 (for only the PA−CMG2 complex), His304, His310, His336 (for only PA), and His597 were successfully determined from their k_{max} values and are listed in Table 2. We could not obtain interpretable sigmoidal curves for the remaining histidine residues mainly because of their slow HDX rates; therefore, the

$t_{1/2}$ values for those histidine residues were calculated from the k obtained at pH* 9.0.

The significant increases in $t_{1/2}$ values due to receptor binding were observed for three histidine residues, His263, His304, and His336, suggesting that their solvent accessibilities decreased upon receptor binding. The increased $t_{1/2}$ value for His263 is probably due to the increased level of stabilization of the local structure against alkaline pH* that occurs upon receptor binding as discussed above. Because His263 and His336 are observed in structures of PA and the PA−CMG2 complex, we compared the solvent accessible surface area (ASA) values for the C_2 atoms of the histidine residues. The ASA values for His263 and His336 in both structures were comparable (His263, 15.5 Å² for PA and 11.1 Å² for the PA−CMG2 complex; His336, 20.3 Å² for PA and 18.1 Å² for the PA−CMG2 complex). Therefore, we cannot explain the results based on the ASA values. This discrepancy may reflect the difference in protein structures in the solution and crystals. The HDX reaction of the C_2 hydrogen of the imidazole group occurs only when the neutral and protonated forms of the imidazole group are in equilibrium and the C_2 atom is in direct contact with water.[23,24] Therefore, the HDX reaction can be diminished when the number of water molecules assisting the acid−base equilibrium of the imidazole group or having contact with the C_2 atom is reduced. Thus, our results indicate that receptor binding tightens the structure of PA, which leads to expelling water molecules around these histidine residues.

Long-Range Stabilization of PA upon CMG2 Binding. Our Gdn-HCl-induced unfolding experiments clearly show that PA is stabilized by CMG2, and the stabilization occurs not only in the domain that directly interacts with CMG2 (His616 located in domain 4) but also in domains that do not have direct contact with CMG2 (His211 and His253 located in domain 1′). Thus, we can safely say that both our combined His-HDX, fluorescence, and protease sensitivity assays indicate that the stabilization afforded by binding of CMG2 occurs up to His211 (which is ∼70 Å from the binding interface) does not seemingly further influence the stability of the PA_{20} domain. Nonetheless, our pH titration study using His-HDX-MS revealed that the microenvironment around histidine residues in PA_{20}, domain 2, and domain 4 changes upon receptor binding. The altered pK_a of His86 in the PA_{20} domain indicates that the binding to CMG2 influences the microenvironment of His86 even though the residue is far from the CMG2 binding interface (>90 Å).

Influence of Receptor Binding on Domain 2 and Domain 4 Dynamics. How does receptor binding influence residues that are far from the binding interface? Previous experiments by Feld and co-workers have indicated that domain 2 and domain 4 are part of a hinge that dictates the oligomeric assembly of PA_{63},[25] such that a tighter interaction favors the formation of heptamers, whereas a weaker interaction may favor the formation of octamers. This implies that domain 2 and domain 4 are capable of hingelike dynamic motions that likely give rise to an overall plasticity in the protein. By anchoring the domain 2−domain 4 interface, hingelike motions are prevented, which in turn would effectively stabilize domain−domain interactions and other noncovalent interactions within the protein.

The PA−CMG2 Complex as a Potential Immunogen in a Future Anthrax Vaccine. PA is the key component of anthrax vaccines currently licensed as well as vaccines under development.[26] Efforts to develop protective adjuvants that do not require the use of a cold chain for storage in areas where a cold chain is not accessible or feasible are ongoing. Our study finds that CMG2 thermodynamically stabilizes PA, and thus, CMG2 may prevent structural perturbations to the protein under long-term storage conditions. Further, the addition of CMG2 slowed the rate of proteolysis by thermolysin. Addition of CMG2 to the vaccine formulation may prevent premature degradation of the protein postinjection, possibly allowing for a greater proportion of PA to ultimately be presented on antigen-presenting cells. Finally, depletion of the actual PA concentration amenable for interacting with the host immune system likely occurs because of the interaction of PA with receptors present on the surface of host cells, and the inclusion of CMG2 in a vaccine formulation should prevent such a depletion of PA.

His-HDX-MS as a Tool To Investigate Protein Stability. Studies have shown that amide HDX in combination with mass spectrometry can be used to provide information about the stability of specific regions within a protein.[27−29] This work demonstrates that His-HDX-MS is complementary to amide HDX, and to other conventional methods such as fluorescence spectroscopy and CD spectroscopy for monitoring protein stability. The advantages of this method over other methods include (1) the ability to follow the side chain stability at a single histidine, which may be more sensitive to the folded state of a protein (because it may be the last part to be stabilized),[30] and to monitor the stabilities of different sites within a protein simultaneously, (2) compared to NMR or CD, the absence of a requirement for large amounts of protein, (3) the fact that proteins do not have to be pure, because mass spectrometry can detect peptide masses even in complex mixtures, and (4) the fact that proteins can be in seemingly any environment, such as a soluble monomer or part of a large oligomeric multiprotein complex within the membrane. These advantages will allow us to study the stabilities of proteins in more complex structures and cellular milieu.

■ ASSOCIATED CONTENT

Ⓢ Supporting Information

Two figures and two tables showing the changes of the solvent (water) concentrations and the His-HDX rates as a function of Gdn-HCl (Figure S1) and the far-UV CD spectrum of WT CMG2 and 4-FTrpCMG2 (Figure S2), a list of histidine-containing peptides used to monitor the Gdn-HCl-induced unfolding of PA (Table S1), and a list of histidine-containing peptides monitored to obtain rate constants (k) of histidine HDX (Table S2). This material is available free of charge via the Internet at http://pubs.acs.org.

■ AUTHOR INFORMATION

Corresponding Authors
*E-mail: jim.bann@wichita.edu.
*E-mail: masaru.miyagi@case.edu.

Notes
The authors declare no competing financial interest.

■ ABBREVIATIONS

CD, circular dichroism; CMG2, capillary morphogenesis protein-2; CHES, *N*-cyclohexyl-2-aminoethanesulfonic acid; FTrp, fluorotryptophan; Gdn-HCl, guanidine hydrochloride; HDX, hydrogen−deuterium exchange; HEPES, 4-(2-hydroxyethyl)-1-piperazineethanesulfonic acid; LC, liquid chromatography; MS, mass spectrometry; NMR, nuclear magnetic resonance; PA, protective antigen; PDB, Protein Data Bank; PF, protection factor; SDS−PAGE, sodium dodecyl sulfate−polyacrylamide gel electrophoresis; TFA, trifluoroacetic acid; VWA, von Willebrand factor A domain.

■ REFERENCES

(1) Klimpel, K. R., Molloy, S. S., Thomas, G., and Leppla, S. H. (1992) Anthrax toxin protective antigen is activated by a cell surface protease with the sequence specificity and catalytic properties of furin. *Proc. Natl. Acad. Sci. U.S.A. 89*, 10277−10281.

(2) Lacy, D. B., Wigelsworth, D. J., Melnyk, R. A., Harrison, S. C., and Collier, R. J. (2004) Structure of heptameric protective antigen bound to an anthrax toxin receptor: A role for receptor in pH-dependent pore formation. *Proc. Natl. Acad. Sci. U.S.A. 101*, 13147−13151.

(3) Kintzer, A. F., Sterling, H. J., Tang, I. I., Abdul-Gader, A., Miles, A. J., Wallace, B. A., Williams, E. R., and Krantz, B. A. (2010) Role of the protective antigen octamer in the molecular mechanism of anthrax lethal toxin stabilization in plasma. *J. Mol. Biol. 399*, 741−758.

(4) Santelli, E., Bankston, L. A., Leppla, S. H., and Liddington, R. C. (2004) Crystal structure of a complex between anthrax toxin and its host cell receptor. *Nature 430*, 905−908.

(5) Bradley, K. A., Mogridge, J., Mourez, M., Collier, R. J., and Young, J. A. (2001) Identification of the cellular receptor for anthrax toxin. *Nature 414*, 225−229.

(6) Varughese, M., Teixeira, A. V., Liu, S., and Leppla, S. H. (1999) Identification of a receptor-binding region within domain 4 of the protective antigen component of anthrax toxin. *Infect. Immun. 67*, 1860−1865.

(7) Wigelsworth, D. J., Krantz, B. A., Christensen, K. A., Lacy, D. B., Juris, S. J., and Collier, R. J. (2004) Binding stoichiometry and kinetics of the interaction of a human anthrax toxin receptor, CMG2, with protective antigen. *J. Biol. Chem. 279*, 23349−23356.

(8) Rajapaksha, M., Lovell, S., Janowiak, B. E., Andra, K. K., Battaile, K. P., and Bann, J. G. (2012) pH effects on binding between the anthrax protective antigen and the host cellular receptor CMG2. *Protein Sci. 21*, 1467−1480.

(9) Scobie, H. M., Marlett, J. M., Rainey, G. J., Lacy, D. B., Collier, R. J., and Young, J. A. (2007) Anthrax toxin receptor 2 determinants that dictate the pH threshold of toxin pore formation. *PLoS One 2*, e329.

(10) Rainey, G. J., Wigelsworth, D. J., Ryan, P. L., Scobie, H. M., Collier, R. J., and Young, J. A. (2005) Receptor-specific requirements for anthrax toxin delivery into cells. *Proc. Natl. Acad. Sci. U.S.A. 102*, 13278−13283.

(11) Chadegani, F., Lovell, S., Mullangi, V., Miyagi, M., Battaile, K. P., and Bann, J. G. (2014) ^{19}F nuclear magnetic resonance and crystallographic studies of 5-fluorotryptophan-labeled anthrax protective antigen and effects of the receptor on stability. *Biochemistry 53*, 690−701.

(12) Miyagi, M., and Nakazawa, T. (2008) Determination of pK$_a$ values of individual histidine residues in proteins using mass spectrometry. *Anal. Chem. 80*, 6481−6487.

(13) Tran, D. T., Banerjee, S., Alayash, A. I., Crumbliss, A. L., and Fitzgerald, M. C. (2012) Slow histidine H/D exchange protocol for thermodynamic analysis of protein folding and stability using mass spectrometry. *Anal. Chem. 84*, 1653−1660.

(14) Wimalasena, D. S., Janowiak, B. E., Lovell, S., Miyagi, M., Sun, J., Zhou, H., Hajduch, J., Pooput, C., Kirk, K. L., Battaile, K. P., and Bann, J. G. (2010) Evidence that histidine protonation of receptor-bound anthrax protective antigen is a trigger for pore formation. *Biochemistry 49*, 6973−6983.

(15) Wimalasena, D. S., Cramer, J. C., Janowiak, B. E., Juris, S. J., Melnyk, R. A., Anderson, D. E., Kirk, K. L., Collier, R. J., and Bann, J. G. (2007) Effect of 2-fluorohistidine labeling of the anthrax protective antigen on stability, pore formation, and translocation. *Biochemistry 46*, 14928−14936.

(16) Rajapaksha, M., Eichler, J. F., Hajduch, J., Anderson, D. E., Kirk, K. L., and Bann, J. G. (2009) Monitoring anthrax toxin receptor dissociation from the protective antigen by NMR. *Protein Sci. 18*, 17−23.

(17) Miyagi, M., Wan, Q., Ahmad, M. F., Gokulrangan, G., Tomechko, S. E., Bennett, B., and Dealwis, C. (2011) Histidine hydrogen-deuterium exchange mass spectrometry for probing the microenvironment of histidine residues in dihydrofolate reductase. *PLoS One 6*, e17055.

(18) Young, T. A., Skordalakes, E., and Marqusee, S. (2007) Comparison of proteolytic susceptibility in phosphoglycerate kinases from yeast and *E. coli*: Modulation of conformational ensembles without altering structure or stability. *J. Mol. Biol. 368*, 1438−1447.

(19) Fraczkiewicz, R., and Braun, W. (1998) Exact and efficient analytical calculation of the accessible surface areas and their gradients for macromolecules. *J. Comput. Chem. 19*, 319−333.

(20) Minks, C., Huber, R., Moroder, L., and Budisa, N. (1999) Atomic mutations at the single tryptophan residue of human recombinant annexin V: Effects on structure, stability, and activity. *Biochemistry 38*, 10649−10659.

(21) Morihara, K., Tsuzuki, H., and Oka, T. (1968) Comparison of the specificities of various neutral proteinases from microorganisms. *Arch. Biochem. Biophys. 123*, 572−588.

(22) Petosa, C., Collier, R. J., Klimpel, K. R., Leppla, S. H., and Liddington, R. C. (1997) Crystal structure of the anthrax toxin protective antigen. *Nature 385*, 833−838.

(23) Vaughan, J. D., Mughrabi, Z. E., and Wu, C. (1970) The kinetics of deuteration of imidazole. *J. Org. Chem. 35*, 1141−1145.

(24) Bradbury, J. H., Chapman, B. E., and Pellegrino, F. A. (1973) Hydrogen-deuterium exchange kinetics of the C-2 protons of imidazole and histidine compounds. *J. Am. Chem. Soc. 95*, 6139−6140.

(25) Feld, G. K., Kintzer, A. F., Tang, I. I., Thoren, K. L., and Krantz, B. A. (2012) Domain flexibility modulates the heterogeneous assembly mechanism of anthrax toxin protective antigen. *J. Mol. Biol. 415*, 159−174.

(26) Chitlaru, T., Altboum, Z., Reuveny, S., and Shafferman, A. (2011) Progress and novel strategies in vaccine development and treatment of anthrax. *Immunol. Rev. 239*, 221−236.

(27) Mazon, H., Marcillat, O., Forest, E., Smith, D. L., and Vial, C. (2004) Conformational dynamics of the GdmHCl-induced molten globule state of creatine kinase monitored by hydrogen exchange and mass spectrometry. *Biochemistry 43*, 5045−5054.

(28) Mazon, H., Marcillat, O., Forest, E., and Vial, C. (2005) Denaturant sensitive regions in creatine kinase identified by hydrogen/deuterium exchange. *Rapid Commun. Mass Spectrom. 19*, 1461−1468.

(29) Konermann, L., Pan, J., and Liu, Y. H. (2011) Hydrogen exchange mass spectrometry for studying protein structure and dynamics. *Chem. Soc. Rev. 40*, 1224−1234.

(30) Frieden, C. (2003) The kinetics of side chain stabilization during protein folding. *Biochemistry 42*, 12439−12446.